NATIONAL AERONAUTICS AND SPACE ADMINISTRATION

Technical Memorandum 33-703

Viking Orbiter 1975 Thrust Vector Control System Accuracy

L. F. McGlinchey

JET PROPULSION LABORATORY

CALIFORNIA INSTITUTE OF TECHNOLOGY

PASADENA, CALIFORNIA

October 15, 1974

PREFACE

The work described in this report was performed by the
Guidance and Control Division of the Jet Propulsion Laboratory.

ACKNOWLEDGMENT

CONTENTS

FIGURES

ABSTRACT

The purpose of the Thrust Vector Control (TVC) System is to point the engine thrust at the vehicle center of mass and thus maintain attitude stability during propulsive maneuvers. This is accomplished by mounting the engine in a two-axis gimbal system. The TVC system then controls the pointing of the engine by closed loop control of two linear actuators which extend or retract and rotate the engine in its gimbal system.

The velocity vector (ΔV) pointing error incurred during a propulsive maneuver is made up of several parts, and the TVC system error is one of these. This error arises because the center of mass and engine thrust are not perfectly aligned.

It is the purpose of this memorandum to assess the magnitude of the TVC system portion of the ΔV pointing error and to provide simplified and linearized models for predicting its magnitude for the various propulsive maneuvers. The accuracy of the linearized analysis is verified using a detailed nonlinear six-degree-of-freedom computer simulation.

The Jet Propulsion Laboratory is responsible for the Viking Orbiter System, which is part of the overall Viking Project managed by the Viking Project Office at Langley Research Center for NASA. The spacecraft will be launched on a Titan III-E/Centaur launch vehicle in August 1975.

I. INTRODUCTION

The purpose of the thrust vector control (TVC) system is to point the engine thrust at the spacecraft center of mass (CM) and thus maintain attitude stability during propulsive maneuvers. Due to various errors, the engine thrust vector will, in general, be moved from its initial position, and the spacecraft velocity change (ΔV) will not be exactly in the direction commanded. The total ΔV error is made up of several components, e.g., commanded turn errors, gyro drifts, etc., and the TVC system error. The TVC system error arises because CM and the engine thrust are not perfectly aligned. This alignment error is comprised of two fundamentally different error sources: (1) CG error, which arises because the position of the actual spacecraft CM and the position of the actual engine center of thrust are not known with complete accuracy; and (2) angular error, which comes from several sources and results from the fact that the direction of the actual engine thrust vector is not known with complete accuracy.

It is not the purpose of this memorandum to assess the magnitude of these alignment errors, but instead to predict the TVC system contribution to the total ΔV pointing error as a function of these alignment errors. In other words, given so much CG error and so much angular error, the analysis presented here will enable the prediction of the TVC system ΔV pointing error.

The analysis presented herein is based on the work originally done during the design of the Mariner Mars 1971 thrust vector control system. The differences are principally due to spacecraft structural dynamics and mass properties, propellant slosh dynamics, and the TVC system hardware implementation.

II. POINTING ERROR DEFINITION

As previously mentioned, the ΔV pointing error is comprised of such errors as gyro-drift error, commanded turn error, and TVC system error. The TVC system error consists of transient and steady-state characteristics. Before developing the TVC system pointing error characteristics, a brief discussion of the basic system operation is necessary. A sketch of the Viking Orbiter 1975 (VO'75) engine gimbal system is shown in Fig. 1. The thrust pointing error can be expressed as

$$\varphi = \theta + \alpha_{CM} \tag{1}$$

where

$\theta \triangleq$ inertial position of the spacecraft as sensed by the inertial reference unit (IRU)

$\alpha_{CM} \triangleq$ entire angular position uncertainty of the engine CM system

The actual physical motion of the gimbal can be expressed as

$$\alpha_G = \alpha_{CM} - \alpha_A \tag{2}$$

where $\alpha_A \triangleq$ total angular error of the engine-gimbal system and including any pre-aim null shift.

Denoting the TVC system steady-state gain by K,

$$\alpha_G = K\theta$$

From Eqs. (1) and (2)

$$\varphi = \frac{1}{K}\left(\alpha_{CM} - \alpha_A\right) + \alpha_{CM} \tag{3}$$

Inspection of Eq. (3) shows that a TVC system with a high DC gain will exhibit a steady-state error that is insensitive to angular errors but allows CM shift (positional) errors to pass unattenuated. In the Viking Orbiter (VO'75) vehicle, as in the case of Mariner Mars 1971 (MM'71) vehicle it is known that the CM will undergo large positional changes so that α_{CM} is the dominant source of error. For this reason, a "trim loop" or "path guidance" loop is employed which, in effect, sets K equal to -1 and Eq. (3) becomes

$$\varphi = \alpha_A \qquad (4)$$

III. TRANSIENT RESPONSE

A. Dynamic Model

To obtain an accurate estimate of TVC system performance, especially during the initial transient, a complete nonlinear simulation must be performed. This has been done, but it is unduly expensive for general accuracy determination. Instead, the TVC system accuracy is determined using linearized models, and the results are checked using the detailed simulation. Fig. 2 shows a simplified block diagram of the TVC system. Here the gyro and integrator in the IRU are modeled by gains only and then mixed with a rate-to-position time constant of T_G. The forward compensator is a gain K_{FC} and path guidance is a single positive feedback lag. All the other lags in the system are lumped into a single time constant T_A associated with the gimbal servo. The torque on the spacecraft is $-K_T (\phi - \alpha_G)$ which acts upon a simple double integrator approximation (rigid-body) of the attitude dynamics.

B. Velocity Vector Error

Equation (1) gives the steady-state thrust pointing error. Using Eq. (2), the following form is obtained:

$$\varphi = \theta + \alpha_G + \alpha_A \qquad (5)$$

This equation is true, in general, and α_G is the physical motion of the gimbal system. Thus, if $\phi(t)$ is defined as the time variation of gimbal angle, φ can be expressed as

$$\varphi(t) \;=\; \theta(t) + \phi(t) + \alpha_A(t) \tag{6}$$

as the general equation.

Let the mass of the vehicle be M, and the magnitude of the engine thrust be T, and assume that these are constant over the duration of the transient. Further, assume small angle nature for $\phi(t)$ and neglect second-order terms. Under these assumptions, the magnitude of the velocity change is

$$\Delta V(t) \;=\; \frac{T}{M}\, t \tag{7}$$

and the component of ΔV normal to the desired direction (side velocity) is given by

$$\Delta V_X(t) \;=\; \frac{T}{M} \int_0^t \varphi(\tau)\, d\tau \tag{8}$$

The pointing error of the ΔV vector is thus approximated by

$$\gamma(t) \;=\; \left| \frac{\Delta V_X(t)}{\Delta V(t)} \right| \tag{9}$$

If $\Delta V_X(t)$ is known, $\gamma(t)$ can be determined by small angle approximation.

Denoting the independent variable of the Laplace transformation by s, Eq. (6) becomes

$$\varphi(s) \;=\; \theta(s) + \phi(s) + \alpha_A(s) \tag{10}$$

and Eq. (8) is

$$\Delta V_X(s) \;=\; \frac{T}{M}\left[\frac{\varphi(s)}{s} \right] \tag{11}$$

Defining

$$H(s) \triangleq \frac{\theta(s)}{\alpha_G(s)}$$ (12)

and using Eq. (2) in transform form yields

$$\varphi(s) = H(s)\,\alpha_{CM}(s) + \phi(s) + \left[1 - H(s)\right]\alpha_A(s)$$ (13)

Further define

$$G(s) \triangleq \frac{\phi(s)}{\alpha_G(s)}$$ (14)

then

$$\varphi(s) = \left[H(s) + G(s)\right]\alpha_{CM}(s) + \left[1 - G(s) - H(s)\right]\alpha_A(s)$$ (15)

and Eq. (11) becomes

$$\Delta V_X(s) = \frac{T}{M}\left[\frac{H(s) + G(s)}{s}\right]\alpha_{CM}(s) + \left[\frac{1 - H(s) - G(s)}{s}\right]\alpha_A(s)$$ (16)

As expected with a linear system, superposition holds and CM positional off-set errors can be treated separately from the angular errors.

C.   Transfer Functions

Referring to Fig. 2, the previously defined transfer functions can be determined:

$$H(s) = \frac{\theta(s)}{\alpha_G(s)}$$

After some manipulation,

$$H(s) = \frac{K_{FG}\left[\dfrac{T_A T_P}{1 - K_{PG}} s^2 + \dfrac{T_P + T_A (1 - K_{PG})}{1 - K_{PG}} s + 1\right]}{D(s)} \qquad (17)$$

where

$$D(s) = \frac{T_P T_A J}{K_T K_G K_{FC} K_A} s^4 + \frac{J\left[T_A (1 - K_{PG}) + T_P\right]}{K_T K_G K_{FC} K_A} s^3$$

$$+ \left[T_P T_G + \frac{J (1 - K_{PG})}{K_T K_G K_{FC} K_A}\right] s^2 + (T_G + T_P) s + 1 \qquad (18)$$

and

$$K_{FG} = \frac{1 - K_{PG}}{K_G K_{FC} K_A} \qquad (19)$$

$$K_{PG} = K_{FC} K_P \qquad (20)$$

$G(s)$ was defined as

$$G(s) = \frac{\phi(s)}{\alpha_G(s)}$$

and from Fig. 2

$$G(s) = \frac{(T_P s + 1)(T_G s + 1)}{D(s)} \qquad (21)$$

D.   Numerical Values

Table 1 gives the values for the parameters for the transient response model for the first midcourse maneuver, first orbit trim, and second orbit trim (post lander release) conditions. As previously mentioned, the TVC system DC gain K_{FG} must be -1 in value; thus

$$K_{PG} = 1 + K_G K_{FC} K_A \cdot \tag{22}$$

Equation (22) is not an exact equality in Table 1, because nearest standard values are used for the TVC select resistor (Ref. 3) which set the forward compensator and path guidance amplifier gains. The last entries in Table 1 are for the torque constant K_T given by the engine thrust-lever arm product. When the first midcourse values are substituted into Eq. (16), side velocity due to CM offset error is

$$\frac{\Delta V_X(s)}{\alpha_{CM}(s)} = \frac{10.406 \, (1.217 \, s + 1)}{0.5762 \, s^4 + 3.446 \, s^3 + 7.086 \, s + 6.860 \, s + 1} \tag{23}$$

and for angular error

$$\frac{\Delta V_X(s)}{\alpha_A(s)} = \frac{1.274 \, (0.5762 \, s^4 + 3.446 \, s^3 - 2.853 \, s^2 - 1.308 \, s + 1)}{s \, (0.5762 \, s^4 + 3.446 \, s^3 + 7.086 \, s + 6.860 \, s + 1)} \tag{24}$$

In a similar manner, when the first orbit trim values are substituted,

$$\frac{\Delta V_X(s)}{\alpha_{CM}(s)} = \frac{15.331 \, (1.217 \, s + 1)}{0.3537 \, s^4 + 2.116 \, s^3 + 8.103 \, s^2 + 6.860 \, s + 1} \tag{25}$$

and for angular error

$$\frac{\Delta V_X(s)}{\alpha_A(s)} = \frac{1.877 \, (0.3537 \, s^4 + 2.116 \, s^3 - 1.836 \, s^2 - 1.308 \, s + 1)}{s \, (0.3537 \, s^4 + 2.116 \, s^3 + 8.103 \, s^2 + 6.860 \, s + 1)} \tag{26}$$

and finally for the second orbit trim condition,

$$\frac{\Delta V_X(s)}{\alpha_{CM}(s)} = \frac{41.391 \, (0.9345 \, s + 1)}{0.5852 \, s^4 + 3.768 \, s^3 + 8.833 \, s^2 + 6.860 \, s + 1} \tag{27}$$

and for angular error

$$\frac{\Delta V_X(s)}{\alpha_A(s)} = \frac{3.726\,(0.5852\,s^4 + 3.768\,s^3 - 1.547\,s^2 - 4.248\,s + 1)}{s\,(0.5852\,s^4 + 3.768\,s^3 + 8.833\,s^2 + 6.860\,s + 1)} \tag{28}$$

These equations are mathematically more tractable when put through a partial fraction expansion. For each condition, a partial fraction expansion will yield equations of the following form:

$$\frac{\Delta V_X(s)}{\alpha_{CM}(s)} = \frac{K_1}{s + a} + \frac{K_2}{s + b} - \frac{Z}{s + w} - \frac{\overline{Z}}{s + \overline{w}} \tag{29}$$

and

$$\frac{\Delta V_X(s)}{\alpha_A(s)} = \frac{T}{Ms} - \frac{K_1}{s + a} - \frac{K_2}{s + b} + \frac{z}{s + w} + \frac{\overline{z}}{s + \overline{w}} \tag{30}$$

where

K_1, K_2, a, b = real constants

Z, w = complex constants

$\overline{Z}, \overline{w}$ = complex conjugate of Z, w

Taking the inverse Laplace transform of Eqs. (29) and (30) will allow the calculation of $\Delta V_X(t)$ for any CM offset and angular error for each of the flight conditions. The ΔV pointing error can then be calculated using Eq. (9). In the time domain, Eqs. (29) and (30) become for unit CM and angular errors

$$\Delta V_{XC}(t) = \frac{K_1}{a}\left(1 - e^{-at}\right) + \frac{K_2}{b}\left(1 - e^{-bt}\right) - \frac{z}{w}\left(1 - e^{-wt}\right)$$

$$- \frac{\overline{z}}{\overline{w}}\left(1 - e^{-\overline{w}t}\right) \tag{31}$$

and

$$\Delta V_{XA}(t) = \Delta V(t) - \frac{K_1}{a}\left(1 - e^{-at}\right) - \frac{K_2}{b}\left(1 - e^{-bt}\right)$$
$$+ \frac{z}{w}\left(1 - e^{-wt}\right) + \frac{\overline{z}}{\overline{w}}\left(1 - e^{-\overline{w}t}\right) \tag{32}$$

The constants in Eqs. (31) and (32) are listed in Table 2 for each of the three flight conditions.

IV. STEADY-STATE ACCURACY

In developing the relationships for transient response error, all parameter values were taken as nominal. This is, of course, the ideal case and with the actual hardware there will be not only tolerances on the gains but cross-coupling of the axes. It is the purpose of this section to estimate these factors and predict the steady-state ΔV pointing error due to the TVC system.

A. Position Gain Equations

Figure 3 shows the position signal path for one axis (pitch or yaw) of the TVC system. Denoting X as pitch and Y as yaw, the pitch and yaw compensator steady-state outputs are

$$V_{AX} = \frac{K_{GY}\, K_{FCX}}{1 - K_{PGX}}\theta_X \tag{33}$$

$$V_{AY} = \frac{K_{GY}\, K_{FCY}}{1 - K_{PGY}}\theta_Y \tag{34}$$

From Fig. 3, it can be seen that the extensions of the gimbal actuators are

$$e_X = \frac{V_{AX}\, K_{DV}}{K_{FBX}} + \frac{V_{PAX}\, K_{PA}}{K_{FBX}} \tag{35}$$

$$e_Y = \frac{V_{AY}\, K_{DV}}{K_{FBY}} + \frac{V_{PAY}\, K_{PA}}{K_{FBY}} \tag{36}$$

where V_{PAX} and V_{PAY} are the pre-aim voltages, and if this bias is separated out,

$$e_X = \delta_X + e_{PX} \tag{37}$$

$$e_Y = \delta_Y + e_{PY} \tag{38}$$

where

$$\delta_X = \frac{V_{AX} K_{DV}}{K_{FBY}} \tag{39}$$

$$\delta_Y = \frac{V_{AY} K_{DV}}{K_{FBY}} \tag{40}$$

and the pre-aim extensions

$$e_{PX} = \frac{V_{PAX} K_{PA}}{K_{FBX}} \tag{41}$$

$$e_{PY} = \frac{V_{PAY} K_{PA}}{K_{FBY}} \tag{42}$$

Combining Eqs. (33), (34), and (39), (40)

$$\delta = \left[K_{FD} \right] \theta \tag{43}$$

with

$$\delta = \mathrm{col} \left\{ \delta_X, \ \delta_Y \right\}$$

$$\theta = \mathrm{col} \left\{ \theta_X, \ \theta_Y \right\}$$

and

$$K_{FD} = \begin{bmatrix} K_X & 0 \\ 0 & K_Y \end{bmatrix} \qquad (44)$$

where

$$K_X = \frac{K_{GY} \, K_{FCX} \, K_{DV}}{(1 - K_{PGX}) \, K_{FBX}} \qquad (45)$$

$$K_Y = \frac{K_{GY} \, K_{FCY} \, K_{DV}}{(1 - K_{PGY}) \, K_{FBY}} \qquad (46)$$

B. Selection of Position Gains

As previously described, the gains are selected for proper path guidance, producing steady-state positions

$$\theta_X = -\alpha_{GX}$$

$$\theta_Y = -\alpha_{GY}$$

θ_X and θ_Y are the attitude rotations about the pitch and yaw axes and α_{GX} and α_{GY} are the components of actual gimbal rotation. For the purpose of gain selection, the gimbal system is considered linear and that

$$\alpha_{G_X} = \frac{-\delta_X}{L_E} \qquad (47)$$

$$\alpha_{G_Y} = \frac{-\delta_Y}{L_E} \qquad (48)$$

with L_E being the lever arm from the actuator clevis to engine center of rotation. Combining Eq. (43) with the approximations (47) and (48) and further assuming that the gimbal system is exactly aligned with the spacecraft XYZ system, yields

$$
\begin{bmatrix} \alpha_{G_X} \\ \alpha_{G_Y} \end{bmatrix} = \begin{bmatrix} \dfrac{-K_X}{L_E} & 0 \\ 0 & \dfrac{-K_Y}{L_E} \end{bmatrix} \begin{bmatrix} \theta_X \\ \theta_Y \end{bmatrix} \tag{49}
$$

To satisfy the path guidance criterion, it is necessary to select

$$
K_X = K_Y = L_E \tag{50}
$$

in order to obtain

$$
\begin{bmatrix} \alpha_{G_X} \\ \alpha_{G_Y} \end{bmatrix} = - \begin{bmatrix} \theta_X \\ \theta_Y \end{bmatrix} \tag{51}
$$

C.   Gain Accuracy

The basic TVC loop mechanization is shown in Fig. 4. Because of the large change in vehicle moments of inertia that occur at lander separation, compensator and path guidance gain changes (via CCS command) are required to maintain system stability. The TVC DC gains as well as the transient response are set using "select resistors" that are located for easy access on top of the modules and on the multilayer board. These resistor values are computed and rounded to nearest standard value by a special computer program. The TVC select resistor values for both flight spacecraft and the proof-test model (PTM)/spare are the same and are listed in Table 3. Using the subscript H to denote high gain (pre-lander release) and L to denote low gain (post lander release), the compensator and path guidance loop gains are

$$K_{FC_L} = \frac{\left[R_{12}(R_{19} + R_{23}) + R_{19}R_{23}\right]}{R_{23}R_6} \tag{52}$$

$$K_{FC_H} = \frac{R_{12}\left[1 + R_{19}\left(\frac{1}{R_{23}} + \frac{1}{R_4} + \frac{1}{R_{12}}\right)\right]}{R_6} \tag{53}$$

$$K_{PG_L} = \frac{R_6 R_{14} K_{FC_L}}{(R_{16} + R_{17})R_9} \tag{54}$$

$$K_{PG_H} = \frac{R_{14} R_6 K_{FC_H}}{R_{16} R_9 \left(2 + \frac{R_{16}}{R_3}\right)} \tag{55}$$

For assessing the accuracy of the gains, the expedient will be used that all error sources are gaussian and independent and worst-case values will be taken as 3σ. The worst-case tolerance on resistor values is taken as ±2 percent. This is made up of an initial tolerance of ±1 percent, a variation due to temperature (100 ppm at 50°C) of ±0.5 percent and a life change of ±0.5 percent. The gain variation from a ±2 percent resistor tolerance was computed for each resistor in Eqs. (52) through (55) and the results root-sum-squared to obtain the total 3σ variation. The results are summarized in Table 4 and include the quoted variations in the IRU position scale factor K_{GY} and the gimbal actuator feedback scale factor K_{FB}. The largest worst-case variation is in K_{FB} and is due to the "soft" supply which generates the LVDT excitation voltage and its variation with LVDT input impedance.

D. Gimbal Transfer Characteristic

The actual gimbal system transfer characteristic which relates gimbal angle and actuator extension is nonlinear and includes inter-axis coupling. This transfer characteristic was originally derived for the MM'71 gimbal system and was repeated for the VO'75 system and the results were used for developing a computer program for determining the computer command subsystem (CCS) pre-aim commands and for developing second-order

approximations for the accuracy analysis. To determine the required gimbal pre-aim, it is necessary to express actuator extensions as a function of gimbal angles. This is done by expressing first the given gimbal rotations in terms of Euler angles and then considering the geometrical constraints in the rotated system. The result is a nonlinear system of the form

$$e_X = g_X (\phi_X, \phi_Y) \tag{56}$$

$$e_Y = g_Y (\phi_X, \phi_Y) \tag{57}$$

However, the reverse problem, to find the gimbal angles when the actuator lengths are given, can only be solved numerically. For the purpose of the accuracy analysis, approximations can be derived. Referring back to Eqs. (37) and (38), ϕ_X and ϕ_Y can be expressed as the result of a Taylor series

$$\phi_X = f_X (e_{PX}, e_{PY}) + \left.\frac{\partial f_X}{\partial e_X}\right|_{\substack{e_{P_X} \\ e_{P_Y}}} \delta_X + \left.\frac{\partial f_X}{\partial e_Y}\right|_{\substack{e_{P_X} \\ e_{P_Y}}} \delta_Y + \theta(\delta^2) \tag{58}$$

and

$$\phi_Y = f_Y \left(e_{P_X}, e_{P_Y}\right) + \left.\frac{\partial f_Y}{\partial e_X}\right|_{\substack{e_{P_X} \\ e_{P_Y}}} \delta_X + \left.\frac{\partial f_Y}{\partial e_Y}\right|_{\substack{e_{P_X} \\ e_{P_Y}}} \delta_Y + \theta(\delta^2) \tag{59}$$

As previously stated, closed-form representations for f_X and f_Y are not known but second-order approximations are

$$\phi_X \approx \frac{-e_X}{L_E} + \frac{e_X^2}{2L_E L_N} + \left(1 + \frac{L_C^2}{L_E^2}\right)\frac{e_Y^2}{2L_E L_N} \tag{60}$$

$$\phi_Y = \frac{-e_Y}{L_E} + \frac{e_Y^2}{2L_E L_N} + \left(1 + \frac{L_C^2}{L_E^2}\right)\frac{e_X^2}{2L_E L_N} + \frac{L_C}{L_E^3} e_X e_Y \qquad (61)$$

with L_N the null length of the actuator and L_C the distance between engine centerline (thrust axis) and the gimbal actuator attach points. Previous analysis has shown that approximating engine rotation by gimbal angle is consistent with the other approximations. Furthermore, the Taylor series will be truncated, and the expressions for gimbal motion become

$$\alpha_{G_X} = \left.\frac{\partial \phi_X}{\partial e_X}\right|_{\substack{e_{P_X} \\ e_{P_Y}}} \delta_X + \left.\frac{\partial \phi_X}{\partial e_Y}\right|_{\substack{e_{P_X} \\ e_{P_Y}}} \delta_Y \qquad (62)$$

$$\alpha_{G_Y} = \left.\frac{\partial \phi_Y}{\partial e_X}\right|_{\substack{e_{P_X} \\ e_{P_Y}}} \delta_X + \left.\frac{\partial \phi_Y}{\partial e_Y}\right|_{\substack{e_{P_A} \\ e_{P_B}}} \delta_Y \qquad (63)$$

Taking the partial derivatives in Eqs. (62) and (63) yields

$$\alpha_{G_X} = \frac{1}{L_E}\left[(a_1 - 1)\, \delta_X + a_2\, \delta_Y\right] \qquad (64)$$

and

$$\alpha_{G_Y} = \frac{1}{L_E}\left[a_3\, \delta_X + (a_4 - 1)\, \delta_Y\right] \qquad (65)$$

where

$$a_1 = \frac{^eP_X}{L_N} \tag{66}$$

$$a_2 = \left(1 + \frac{L_C^2}{L_E^2}\right)\frac{^eP_Y}{L_N} \tag{67}$$

$$a_3 = \frac{^eP_X}{L_N}\left(1 + \frac{L_C^2}{L_E^2}\right) + \frac{L_C}{L_E^2}\,{}^eP_Y \tag{68}$$

$$a_4 = \frac{^eP_Y}{L_N} + \frac{L_C}{L_E^2}\,{}^eP_X \tag{69}$$

Substituting the values

$$L_E = 6.43 \text{ cm } (2.53 \text{ in.})$$

$$L_C = 8.26 \text{ cm } (3.25 \text{ in.})$$

$$L_N = 17.2 \text{ cm } (6.763 \text{ in.})$$

will yield the values of α_{G_X} and α_{G_Y} as functions of the pre-aim. For Mission B, the presently predicted values are listed in Table 5. Substitution of these values into Eqs. (66) through (69) will yield the coefficients for the gimbal motion Eqs. (64) and (65) and are listed in Table 5.

Another source of error is that the gimbal reference axes will not be exactly aligned with the IRU sensed axes. Let the misalignment rotation be γ radians so that

$$
\begin{bmatrix} \theta_{X_s} \\ \theta_{Y_s} \end{bmatrix} = \begin{bmatrix} \cos \gamma & -\sin \gamma \\ \sin \gamma & \cos \gamma \end{bmatrix} \begin{bmatrix} \theta_X \\ \theta_Y \end{bmatrix} \tag{70}
$$

and via small angle approximations

$$
\begin{bmatrix} \theta_{X_s} \\ \theta_{Y_s} \end{bmatrix} = \begin{bmatrix} 1 & -\gamma \\ \gamma & 1 \end{bmatrix} \begin{bmatrix} \theta_X \\ \theta_Y \end{bmatrix} \tag{71}
$$

The 3σ estimate for γ is taken as 5 mrad.

E.   Steady-State Thrust Pointing Accuracy

In Section IV-B it was shown that to satisfy the path guidance criterion, it is necessary to select the forward gains

$$
K_X = K_Y = L_E
$$

with L_E being the lever arm from the actuator clevis to engine center of rotation. Estimates of the 3σ errors in the various gains which make up K_X and K_Y were developed in Section IV-C and are listed in Table 4. Applying these errors to Eqs. (45) and (46) and computing the RSS total gives a 3σ value of 0.24 for K_X and K_Y. To determine the total steady-state error, first let

$$
K_X = L_E (1 + e_1) \tag{72}
$$

and

$$
K_Y = L_E (1 + e_2) \tag{73}
$$

so that combining with Eqs. (64), (65), and (71) gives

$$
\begin{bmatrix} {}^{\alpha}G_X \\ {}^{\alpha}G_Y \end{bmatrix} = \frac{1}{L_E} \begin{bmatrix} (a_1 - 1) & a_2 \\ a_3 & (a_4 - 1) \end{bmatrix} \begin{bmatrix} L_E (1 + e_1) & 0 \\ 0 & L_E (1 + e_2) \end{bmatrix} \begin{bmatrix} 1 & -\gamma \\ \gamma & 1 \end{bmatrix} \begin{bmatrix} \theta_X \\ \theta_Y \end{bmatrix}
$$

$$(74)$$

Expanding Eq. (74) and neglecting second-order terms and higher yields

$$
\begin{bmatrix} {}^{\alpha}G_X \\ {}^{\alpha}G_Y \end{bmatrix} = \begin{bmatrix} -(1 - a_1 + e_1) & a_2 + \gamma \\ a_3 - \gamma & -(1 - a_4 + e_2) \end{bmatrix} \begin{bmatrix} \theta_X \\ \theta_Y \end{bmatrix}
$$

$$(75)$$

and using the identity matrix $[I]$ becomes

$$
\begin{bmatrix} {}^{\alpha}G_X \\ {}^{\alpha}G_Y \end{bmatrix} = - \begin{bmatrix} I + K \end{bmatrix} \begin{bmatrix} \theta_X \\ \theta_Y \end{bmatrix}
$$

$$(76)$$

where the elements of K are

$$K_{11} = e_1 - a_1 \tag{77}$$

$$K_{12} = - (a_2 + \gamma) \tag{78}$$

$$K_{21} = - (a_3 - \gamma) \tag{79}$$

$$K_{22} = e_2 - a_4 \tag{80}$$

Rewriting Eq. (76) as

$$\begin{bmatrix} \theta_X \\ \theta_Y \end{bmatrix} = - \begin{bmatrix} I + K \end{bmatrix}^{-1} \begin{bmatrix} {}^\alpha G_X \\ {}^\alpha G_Y \end{bmatrix} \qquad (81)$$

yields again to first order

$$\begin{bmatrix} \theta_X \\ \theta_Y \end{bmatrix} = - \begin{bmatrix} I - K^T \end{bmatrix} \begin{bmatrix} {}^\alpha G_X \\ {}^\alpha G_Y \end{bmatrix} \qquad (82)$$

The vector form of the steady-state pointing error Eq. (5) is

$$\begin{bmatrix} \varphi_X \\ \varphi_Y \end{bmatrix} = \begin{bmatrix} \theta_X \\ \theta_Y \end{bmatrix} + \begin{bmatrix} {}^\alpha G_X \\ {}^\alpha G_Y \end{bmatrix} + \begin{bmatrix} {}^\alpha A_X \\ {}^\alpha A_Y \end{bmatrix} \qquad (83)$$

Substituting Eq. (82) into (83) gives

$$\begin{bmatrix} \varphi_X \\ \varphi_Y \end{bmatrix} = \begin{bmatrix} K \end{bmatrix}^T \begin{bmatrix} {}^\alpha G_X \\ {}^\alpha G_Y \end{bmatrix} + \begin{bmatrix} {}^\alpha A_X \\ {}^\alpha A_Y \end{bmatrix} \qquad (84)$$

Equation (2) can now be used to produce

$$\begin{bmatrix} \varphi_X \\ \varphi_Y \end{bmatrix} = \begin{bmatrix} K \end{bmatrix}^T \begin{bmatrix} \alpha_{CM_X} \\ \alpha_{CM_Y} \end{bmatrix} + \begin{bmatrix} I - K^T \end{bmatrix} \begin{bmatrix} \alpha_{A_X} \\ \alpha_{A_Y} \end{bmatrix} \qquad (85)$$

Equation (81) is now used to estimate the steady-state pointing error. Separating CM and angular errors and expanding yields for CM errors

$$\varphi_{CM_X} = K_{11} \, \alpha_{CM_X} + K_{21} \, \alpha_{CM_Y} \qquad (86)$$

$$\varphi_{CM_Y} = K_{12} \, \alpha_{CM_X} + K_{22} \, \alpha_{CM_Y} \qquad (87)$$

and for angular errors

$$\varphi_{A_X} = (1 - K_{11}) \, \alpha_{A_X} - K_{21} \, \alpha_{A_Y} \qquad (88)$$

$$\varphi_{A_Y} = - K_{12} \, \alpha_{A_X} + (1 - K_{22}) \, \alpha_{A_Y} \qquad (89)$$

A CM offset error of α_{CM} and an angular error of α_A divide according to

$$\alpha_{CM_X} = \alpha_{CM} \sin (\Omega)$$

$$\alpha_{CM_Y} = \alpha_{CM} \cos (\Omega)$$

$$\alpha_{A_X} = \alpha_A \sin (\Gamma)$$

$$\alpha_{A_Y} = \alpha_A \cos (\Gamma)$$

where Ω and Γ are assumed independent random variables uniformly distributed 0 to 2π. Recalling that e_1 and e_2 in Eqs. (77) through (80) are

gaussian random variables with a 3σ value of 0.24, and that the total pointing error is

$$\varphi = \sqrt{\varphi_X^2 + \varphi_Y^2} \tag{90}$$

the steady-state CM offset and angular errors can now be computed. This was done using a Monte Carlo technique on the digital computer. The results are given in the form

$$\left(\varphi_{CM}\right)_{ss} = (M_C \pm 3\sigma_C)\, \alpha_{CM} \tag{91}$$

$$\left(\varphi_A\right)_{ss} = (M_A \pm 3\sigma_A)\, \alpha_A \tag{92}$$

where

$\qquad M_C,\ \sigma_C \triangleq$ mean and standard deviation of the steady-state pointing
$\qquad\qquad\qquad$ error due to a unit CM offset

and

$\qquad M_A,\ \sigma_A =$ mean and standard deviation of the steady-state pointing
$\qquad\qquad\qquad$ error due to a unit angular error

The mean and 3σ values in Eqs. (91) and (92) are given in Table 6.

V.   TOTAL TVC SYSTEM POINTING ERROR

A.   Combining Transient and Steady-State Errors

The $\Delta V_X(t)$ functions necessary to compute the transient pointing error were derived in Section III-D and are given by Eqs. (31) and (32) and Table 2. The form of the TVC system transient pointing error is given by Eq. (9). For a unit CM offset error, let

$$P_C(t) \triangleq \left| \frac{\Delta V_{XC}(t)}{\Delta V(t)} \right| \tag{93}$$

and for a unit angular error

$$P_A(t) \triangleq \left| \frac{\Delta V_{XA}(t)}{\Delta V(t)} \right| \tag{94}$$

Equations (93) and (04) can be solved in the digital computer using the complex arithmetic capability of Fortran. This was done, and the resulting time functions are depicted in Figs. 5 through 16. Figures 5 and 6 give $P_C(t)$ for the first midcourse maneuver. They are identical except that Fig. 5 is an expansion of the first 25 seconds of Fig. 6. Similarly, Figs. 7 and 8 show $P_A(t)$ for the first midcourse maneuver. For the first orbit trim, Figs. 9 and 10 give $P_C(t)$ and Figs. 11 and 12 give $P_A(t)$, and for the second orbit trim following lander separation, Figs. 13 and 14 give $P_C(t)$ and Figs. 15 and 16 give $P_A(t)$.

Since ideal path guidance is implicit, $P_A(t)$ approaches unity asymptotically and $P_C(t)$ approaches zero (see Section II). To include the steady-state errors computed in Section IV, it is only necessary to combine Eqs. (91) and (92) with (93) and (94) to give

$$\gamma_{CM}(t) = \left[P_C(t) + M_C \pm 3\sigma_C \right] \alpha_{CM} \tag{95}$$

$$\gamma_A(t) = \left[P_A(t) (M_A \pm 3\sigma_A) \right] \alpha_A \tag{96}$$

The transient plus steady-state error for each flight condition can now be computed using Eqs. (95) and (96) in conjunction with Figs. 5 through 16 and the statistical data given in Table 6.

B.   Verification

A complete nonlinear simulation of the TVC system has been written in CSSL[1] III for the Univac 1108 computer and includes the following:

(1)   Six degrees-of-freedom

(2)   Simulation of actual TVC electronics

---

[1]Continuous Systems Simulation Language.

(3)   Spacecraft structural flexibility using hybrid coordinates

(4)   Propellant slosh dynamics modeled using a mechanical pendulum analogy

For direct comparison with Figs. 5, 9, and 13, typical runs with an initial 1.0-degree CM offset for the first midcourse maneuver, first orbit trim, and post-VLCA^2 release are shown in Figs. 17, 18, and 19. In each run, the structural and propellant slosh damping are set at their 3σ lower limits. Comparison of these figures shows nearly exact agreement with the nonlinear simulation and thus verifies the accuracy of the foregoing analysis. The somewhat oscillatory behavior in the simulation results is due to the disturbances introduced by propellant slosh dynamics.

VI.   SUMMARY

Given estimates of the total CM offset in degrees and the total angular error in degrees, the ΔV pointing error due to the thrust vector control system can be estimated by using Eqs. (95) and (96) and the statistical data in Table 6. For the first midcourse maneuver the results are:

$$\gamma_{CM}(t) = \left[P_C(t) + 0.071 \pm 0.13\right] \alpha_{CM} \tag{97}$$

$$\gamma_A(t) = \left[P_A(t) (1.00 \pm 0.21)\right] \alpha_A \tag{98}$$

where $P_C(t)$ is given in Fig. 5 or 6 and $P_A(t)$ in Fig. 7 or 8. The ($\pm$) terms are the possible 3σ variations. For the first orbit trim,

$$\gamma_{CM}(t) = \left[P_C(t) + 0.068 \pm 0.13\right] \alpha_{CM} \tag{99}$$

$$\gamma_A(t) = \left[P_A(t) (1.00 \pm 0.21)\right] \alpha_A \tag{100}$$

where $P_C(t)$ is given in Fig. 9 or 10 and $P_A(t)$ in Fig. 11 or 12.

---

^{2}Viking launch capsule.

Finally, for the second orbit trim,

$$\gamma_{CM}(t) = \left[P_C(t) + 0.082 \pm 0.14\right]\alpha_{CM} \qquad (101)$$

$$\gamma_A(t) = \left[P_A(t)(1.04 \pm 0.22)\right]\alpha_A \qquad (102)$$

where $P_C(t)$ is given in Fig. 13 or 14 and $P_A(t)$ in Fig. 15 or 16. Alternately, $P_C(t)$ and $P_A(t)$ in the above equations may be solved on the computer in the manner described in Section V-A. The above equations may be used for Mission A or Mission B and for other maneuvers within each mission phase, since the TVC system electrical parameters are identical for the two spacecraft, and differences in mass properties are small.

Table 1. TVC system parameters

Parameters	First midcourse maneuver	First orbit trim	Second orbit trim
Engine thrust T, N (lbf)	1334.47 (300.0)	1334.47 (300.0)	1334.47 (300.0)
Spacecraft mass M, kg (slugs)	3437.59 (235.55)	2332.54 (159.83)	1174.96 (80.51)
TVC forward gain K_G K_{FC} K_A	3.333	3.333	1.105
Lever arm L, m (ft)	1.927 (6.323)	2.38 (7.82)	1.37 (4.506)
Path guidance time constant T_p, s	4.86	4.86	4.86
Rate to position time constant T_G, s	2.0	2.0	2.0
Gimbal servo lag T_A, s	0.15	0.15	0.15
Spacecraft moment of inertia J, kg-m^2 (slug-ft^2)	6775.0 (4997)	5144.0 (3794)	1626.0 (1199)
Path guidance loop gain K_{PG}, V/V	4.328	4.328	2.101
Torque constant K_T, N-m (ft-lb/rad)	2571.85 (1896.90)	3180.75 (2346.00)	1832.79 (1351.8)

Table 2. Constants for computing transient pointing error

Constant	First midcourse maneuver	First orbit trim	Second orbit trim
K_1	1.748	2.912	8.688
K_2	3.102	0.303	0.731
a	0.175	0.184	0.188
b	3.298	0.878	1.108
z	2.425 - j1.855	1.608 + j1.050	4.710 + j8.586
w	1.254 + j1.200	2.460 + j3.387	2.572 + j1.269
$\bar{z}$	2.425 + j1.855	1.608 - j1.050	4.710 - j8.586
$\bar{w}$	1.254 - j1.200	2.460 - j3.387	2.572 - j1.269

Table 3. Select resistors for setting gains

Resistor	Pitch	Yaw
R_1	--	909.0
R_2	--	2.37
R_3	866.0	--
R_4	2.37	--
R_6	221.0	210.0
R_8	267.0	255.0
R_9	110.0	107.0
R_{16}	806.0	806.0
R_{17}	806.0	806.0
R_{19}	10.0	10.0
R_{23}	10.0	10.0

1. All values in kΩ.

2. Complete list in Ref. 3.

Table 4. Gains and tolerances

Gain	Value	Tolerance
K_{GY}	170.5 V/rad	±5.5%
K_{FC_L}	1.041 V/V	±3.0%
K_{FC_H}	3.141 V/V	±3.58%
K_{PG_L}	2.101 V/V	±5.0%
K_{PG_H}	4.328 V/V	±6.27%
K_{DV}	0.068 mA/V	±2.0%
K_{FB}	10.97 cm/V (4.317 in./V)	±20.8%

Table 5. Pre-aim values and coefficients for gimbal motion equations

Maneuver (Mission B)	^{e}PX, m (in.)	^{e}PY, m (in.)	a_1	a_2	a_3	a_4
First midcourse	0. 00215 (0. 00847)	-0. 00122 (-0. 04802)	0. 00125	-0. 0188	-0. 0211	-0. 00280
First orbit trim	0. 000287 (0. 01130)	-0. 000287 (-0. 01130)	0. 00167	-0. 00443	-0. 00131	0. 00407
Second orbit trim	0. 00309 (0. 12146)	-0. 00359 (-0. 01412)	0. 018	-0. 00553	0. 0404	0. 0596

Table 6. Steady-state pointing error statistics

Maneuver	CM offset		Angular error	
	M_C	$3\sigma_C$	M_A	$3\sigma_A$
First midcourse	0.071	0.13	1.00	0.21
First orbit trim	0.068	0.13	1.00	0.21
Second orbit trim	0.082	0.14	1.04	0.22
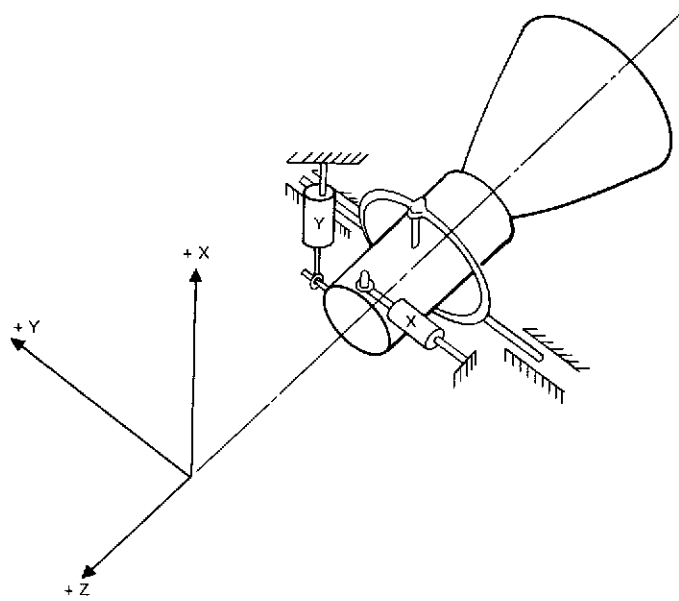
Fig. 1.   Engine and gimbal
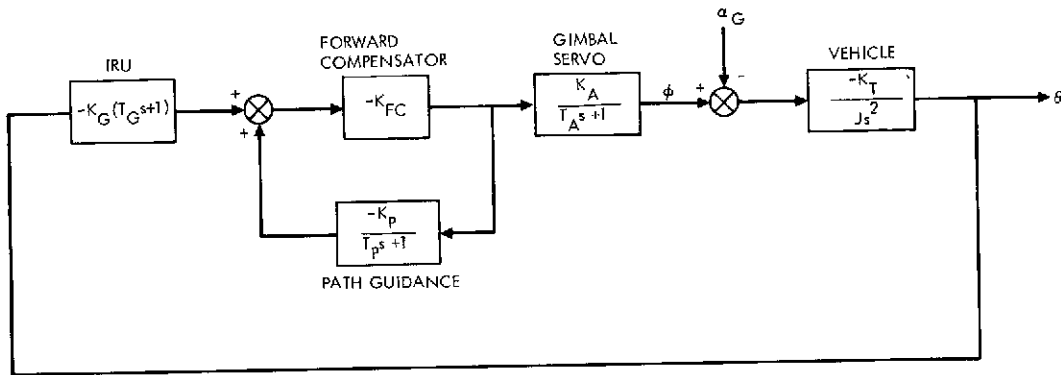
Fig. 2.   Single-axis linearized TVC system block diagram
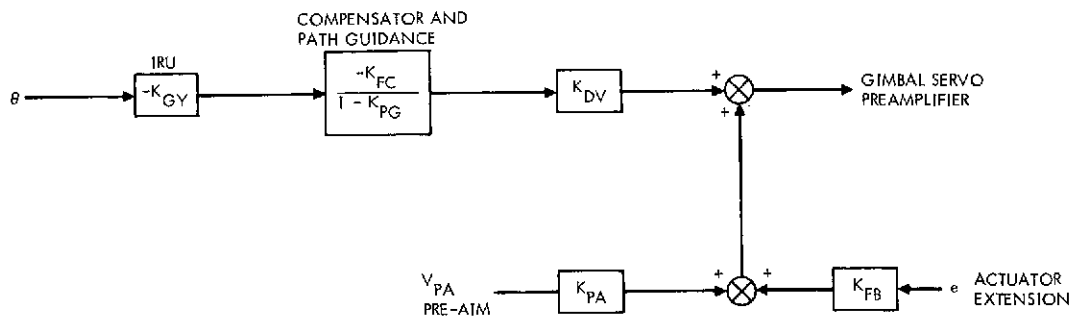
Fig   3.   TVC system signal flow path
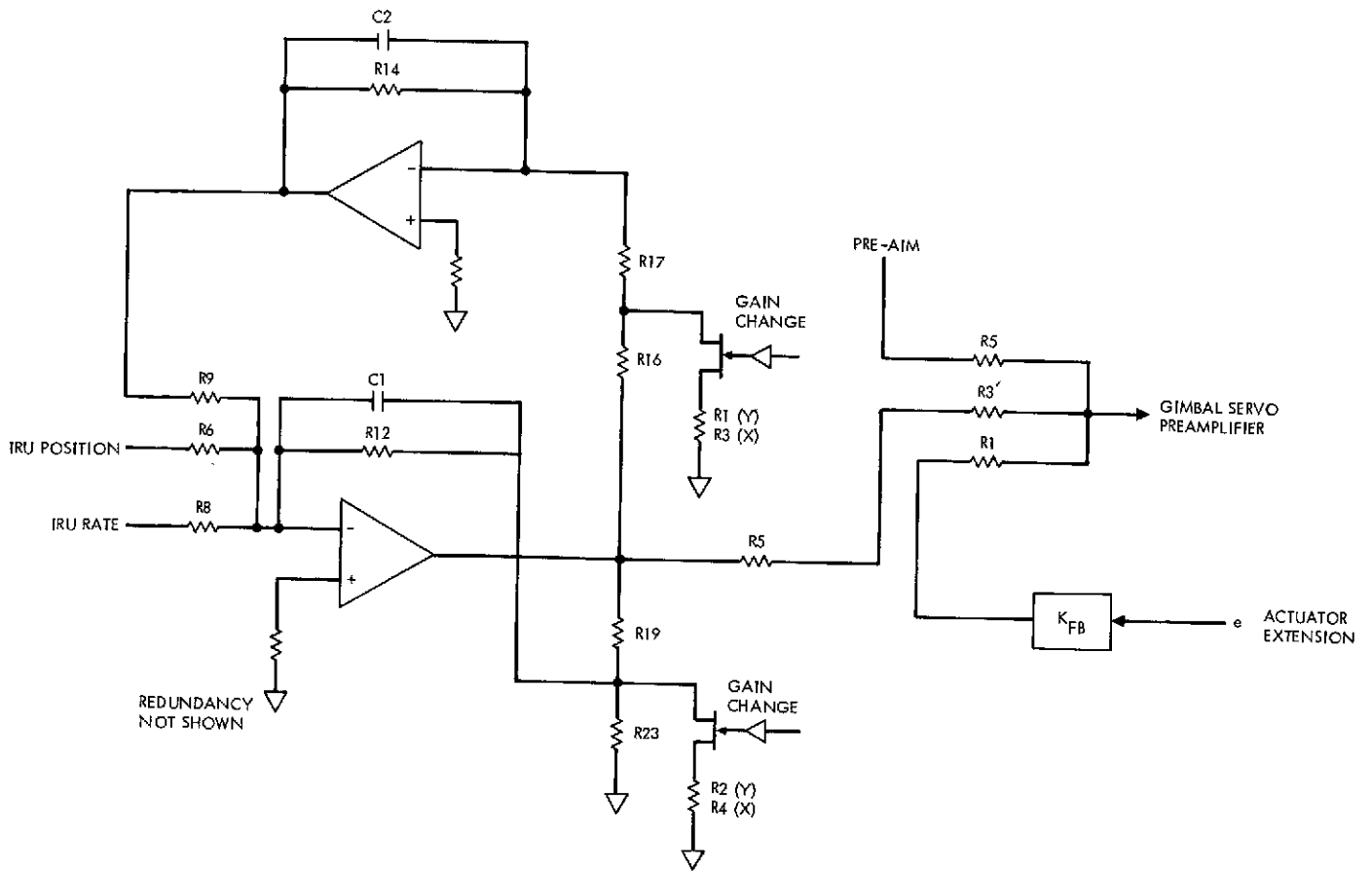
Fig. 4. TVC loop mechanization
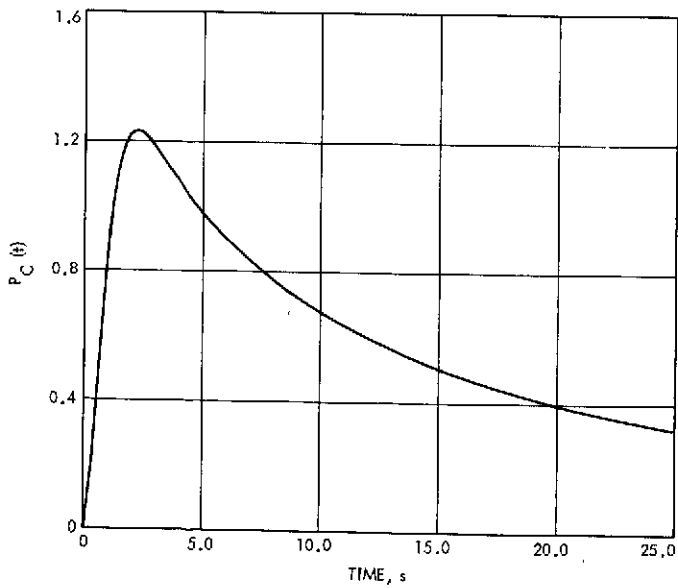
Fig. 5. Pointing error due to CM offset, first midcourse maneuver, 0 to 25 s
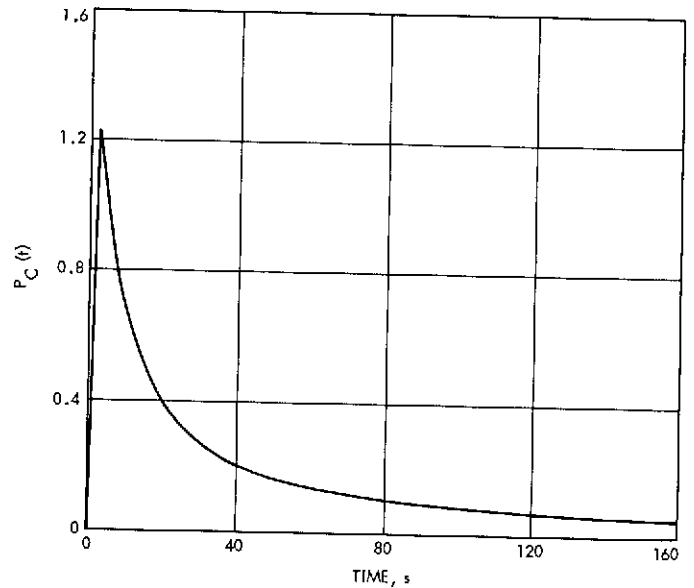
Fig. 6. Pointing error due to CM offset, first midcourse maneuver, 0 to 160 s
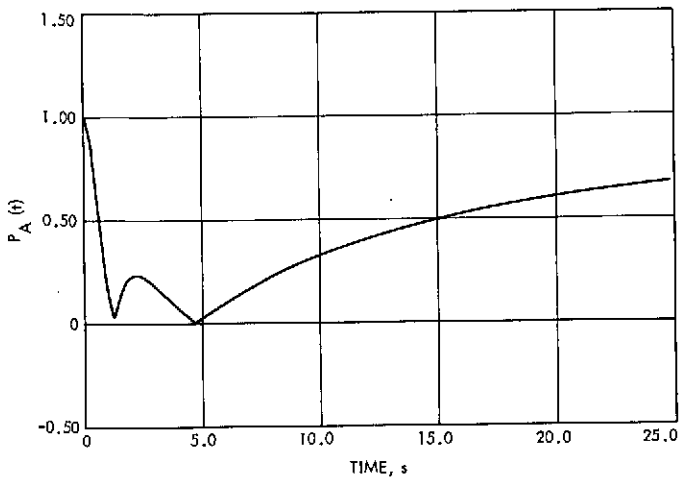
Fig. 7. Pointing error due to angular error, first midcourse maneuver, 0 to 25 s
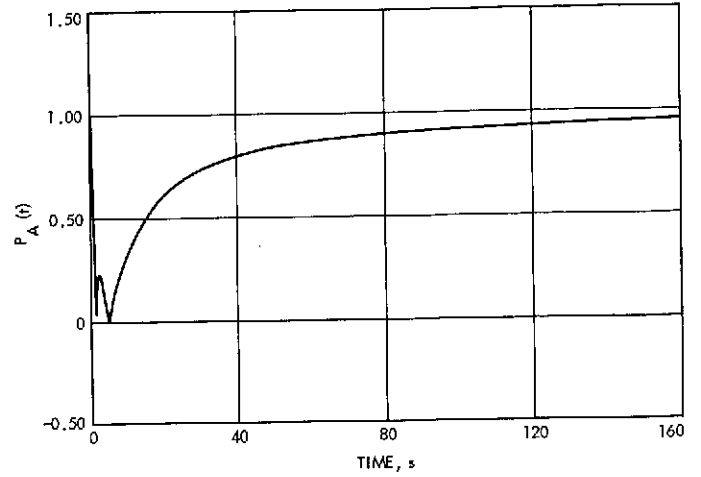
Fig. 8. Pointing error due to angular error, first midcourse maneuver, 0 to 160 s
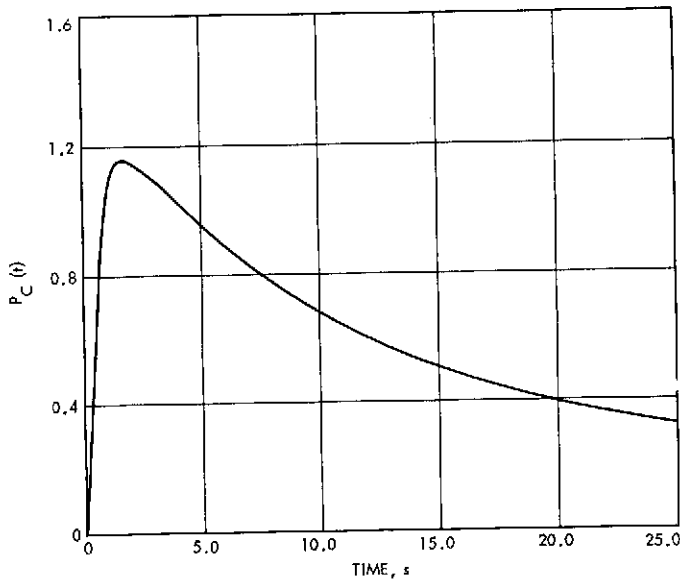
Fig. 9. Pointing error due to CM offset, first orbit trim, 0 to 25 s
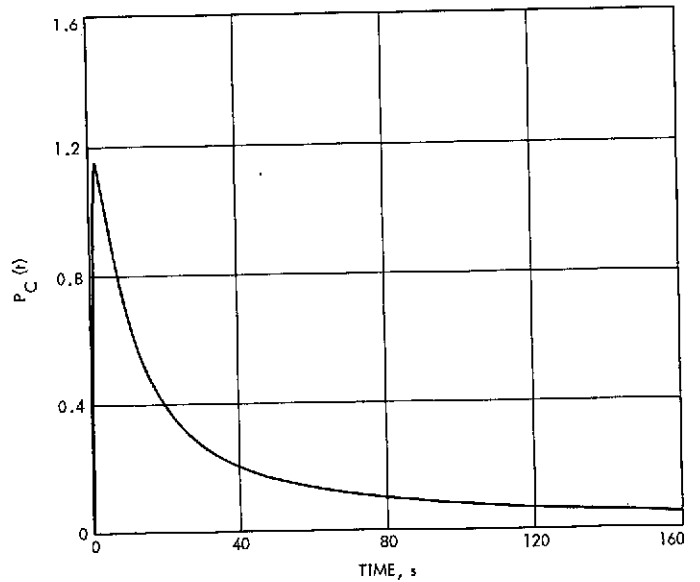
Fig. 10. Pointing error due to CM offset, first orbit trim, 0 to 160 s
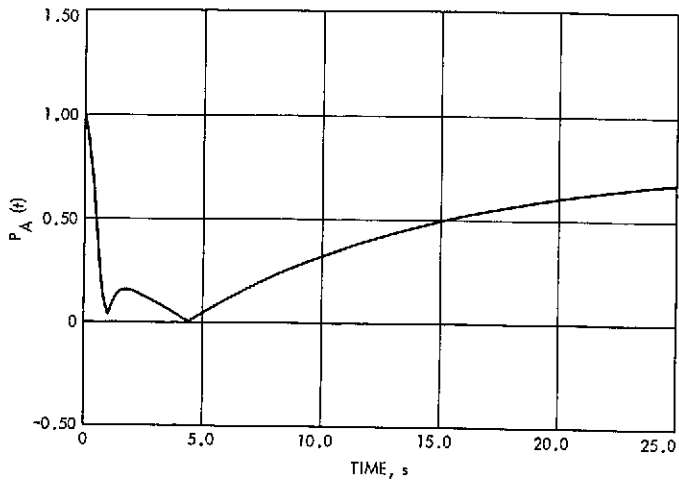
Fig. 11. Pointing error due to angular error, first orbit trim, 0 to 25 s
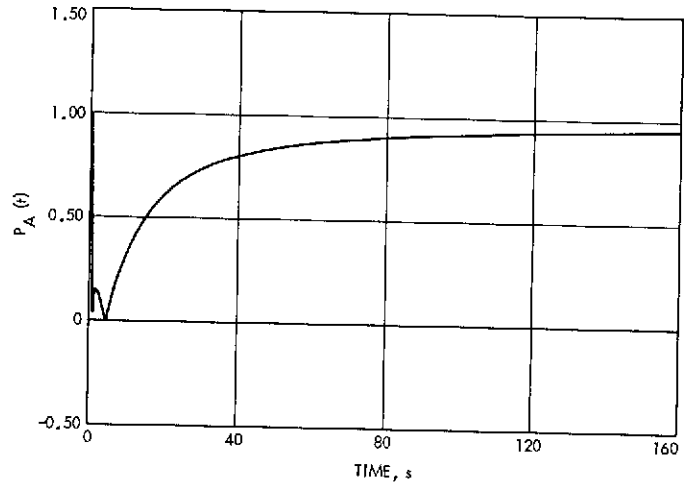
Fig. 12. Pointing error due to angular error, first orbit trim, 0 to 160 s
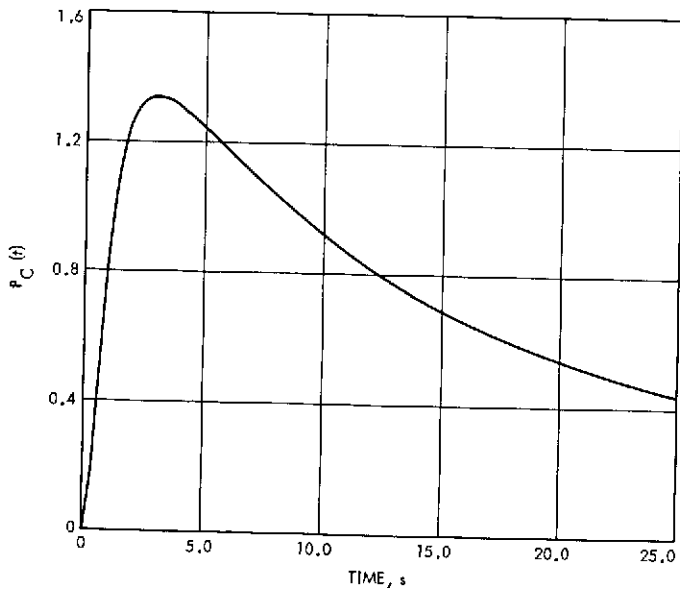
Fig. 13. Pointing error due to CM offset, post VLCA release, 0 to 25 s
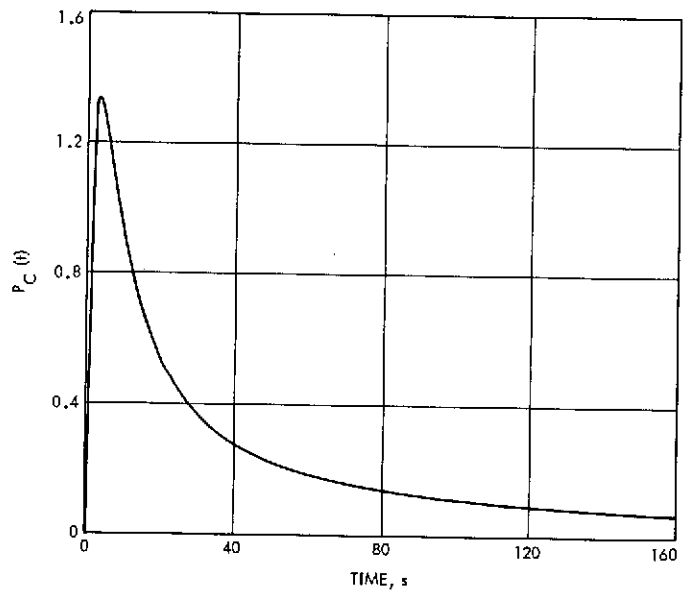
Fig. 14. Pointing error due to CM offset, post VLCA release, 0 to 160 s

34
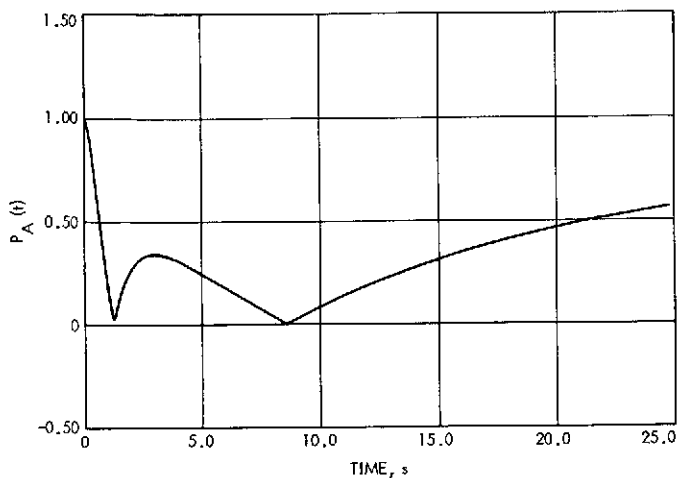
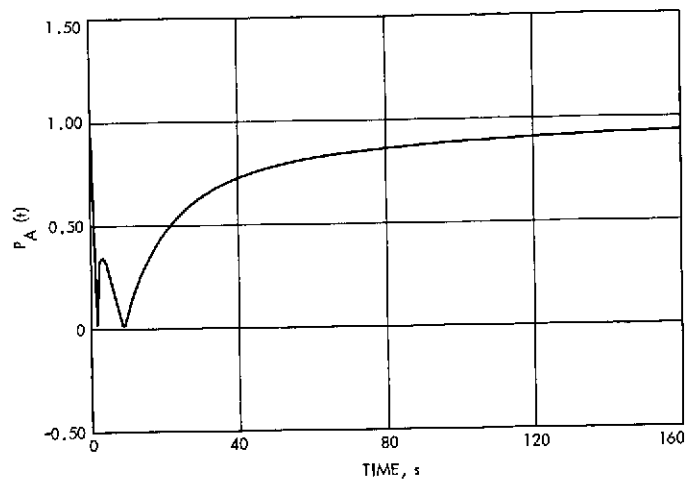Fig. 15. Pointing errors due to angular error, post VLCA release, 0 to 25 s

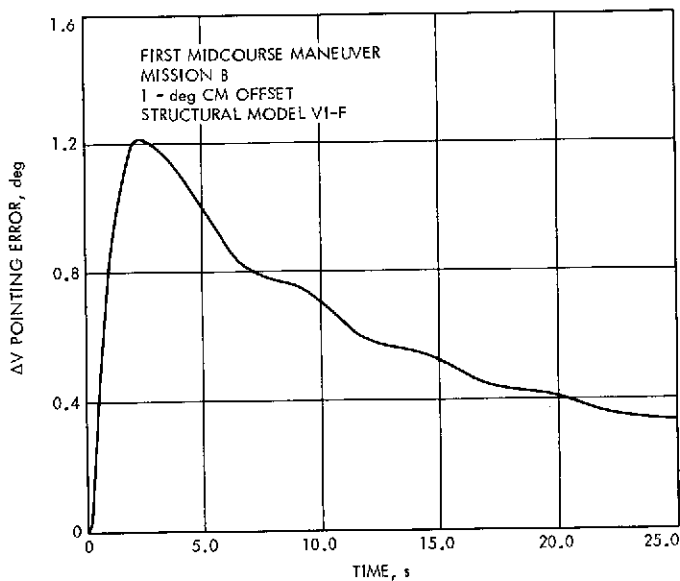Fig. 16. Pointing errors due to angular error, post VLCA release, 0 to 160 s

Fig. 17. ΔV pointing error, first midcourse maneuver, Mission B, 1-deg CM offset, structural Model VI-F
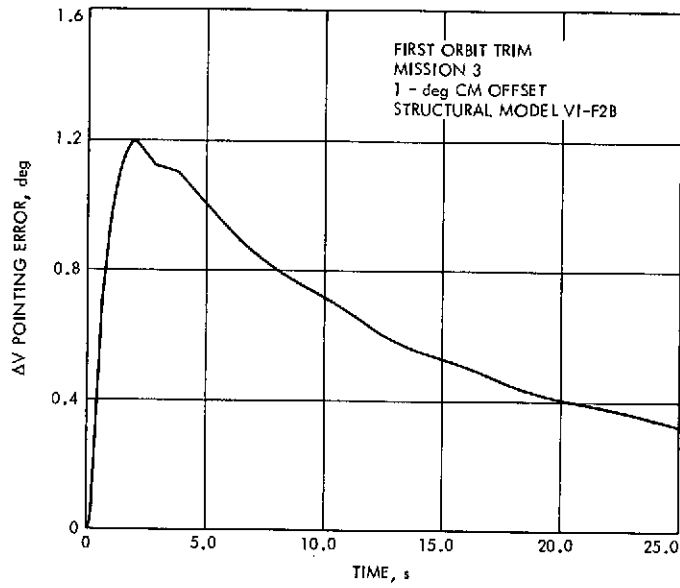
Fig. 18. ΔV pointing error, first orbit
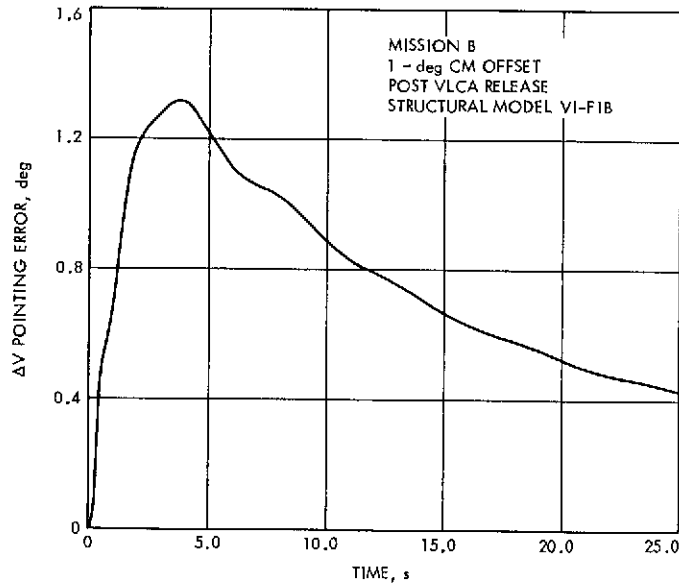trim, Mission B, 1-deg CM offset,
post-VLCA release, structural
Model VI-F1B

Fig. 19. ΔV pointing error,
post-VLCA release